

# Modeling Train Movement for Moving-Block Railway Network Using Cellular Automata

Yonghua Zhou<sup>1</sup> and Chao Mi<sup>1</sup>

**Abstract:** Cellular automata (CAs), model the dynamics of complex systems as the state update of cells restricted from their own neighbors. This paper regards the tempo-spatial constraints as dummy neighborhoods of cells for train movement, such as scheduled movement authority and speed restriction, equivalent to the maximum displacements during the future certain time steps and each time step, respectively. Under the framework of CA modeling, this paper attempts to propose an improved CA model for moving-block railway network which incorporates the tempo-spatial constraints to capture the restrictive, synergistic and autonomous dynamics. We divide the one-dimensional cell lattice into several segments, called instantaneous movement authority, with individual speed restriction and target speed. The physical law controlling train movement is gradually implemented on the segmented lattice. The simulation based on the proposed CA model can reconstruct the phenomenon observed in realistic train movement, such as go-and-stop wave, its back propagation to the upstream, tracking and feedback adjustment. The applicability and rationality of the proposed model has been elucidated through various simulation tests. The model of train movement based on CAs can facilitate finding out the plans to improve the performance of railway network.

**Keywords:** Cellular automata, rail traffic flow, modeling, moving-block system, scheduling and control

## 1 Introduction

Cellular automaton (CA), one kind of computational models, can reproduce and predict the dynamics of complex systems with physical and biological movements. It was first explored in the late 1940s by von Neumann and Ulam [von Neumann (1996)] who attempted to design self-replicating artificial systems analogous to human brains. Hitherto, it has been applied to describe the movement law of com-

---

<sup>1</sup> School of Electronic and Information Engineering, Beijing Jiaotong University, Beijing, P. R. China

plex systems, and reveal various natural phenomena and human behavior, such as cloud formation [Nagel and Raschke (1992)], traffic-flow propagation [Nagel and Schreckenberg (1992); Chowdhury, Wolf, and Schreckenberg (1997); Chowdhury, Santen, and Schadschneider (2000); Meng, Dai, Dong, and Zhang (2007)], pedestrian behaviors [Blue and Adler (2001)], evacuation and panic dynamics [Alizadeh (2011)], etc.

In the CA model, the discrete universe consists of one or multiple-dimensional lattice with finite state machines, called cells. They are locally interconnected with each other. Based on the states of their neighboring cells and the local update rules, all cells synchronously undertake state transition. When all cells utilize the same update rules, the reproduced system will be homogeneous like many realistic physical and biological systems. Based on these ideas, from the viewpoint of statistical mechanics in physics discipline, various traffic CA models have been proposed to replicate macroscopic phenomena through the description of interactions among microscopic hopping particles (vehicles) on the grid. The one-dimensional probabilistic NaSch model is one kind of basic and important description to simulate road traffic, through which the spontaneous emergence of traffic jams can be observed [Maerivoet and Moor (2005)].

Based on the deterministic NaSch traffic model, the CA model was proposed for railway traffic, and the observed complex phenomena can be reproduced in the realistic moving- and fixed-block control systems [Li, Gao, and Ning (2005a, 2005b); Ning, Li, and Gao (2005)]. Afterwards, Zhou, Gao and Li (2006) put forward a CA model for the moving-like block system to investigate the effects of main facts such as the length of location unit, train time interval and initial delay on the delay propagation. The unified CA model was presented to capture the characteristics of driver reaction and minimum time headway [Li, Gao, and Yang (2007); Tang and Li (2007)]. Li, Gao, and Li (2007) proposed the CA model for the four-aspect fixed-block systems. Xun, Ning, and Li (2007) presented the train-following cellular automata model for the moving-block system. Fu, Gao, and Li (2007) brought forward the CA model for the speed-limit sections in the four-aspect fixed-block system. Xun, Ning, and Li (2009) proposed a new CA model to simulate the rail transit system at station. Li, Gao, and Mao (2007) explored the train movement under energy-optimal control strategies.

Train movement can be described in time-based [Higgins and Kozan (1998); Chou, Xia, and Kayserb (2007); Li and Gao (2007)] and event-based ways [Ho, Mao, and Yang (1998); Cheng (1998); Lu, Dessouky, and Leachman (2004); Grube, Núñez, and Cipriano (2011)]. The time-based approach concerns more about the detailed process of train movement in each time interval, while the event-based one focuses on the dynamic response to related discrete events. In terms of modeling tools, the

dynamics of train movement can be represented through the mathematical model such as state-space equations, and the rule-based model such as cellular automata. The state-space equations are suitable for the real-time control of individual train with accurate depiction of its movement. However, the CAs, whose states at next instant are determined by the current states of themselves and their neighbors, more emphasizes the description of the restricted and interdependent movements among trains.

The fundamental physical principles to maneuver train movement are the Newton's second law and the relationship between work of external force and dynamic energy. However, in practice more tempo-spatial constraints will be enforced on train movement especially under the environment of physical network where conflict or collision as well as speed restriction might happen. This paper attempts to propose more generalized CA model in order to delineate the restrictive, cooperative and autonomous tempo-spatial morphologies which commonly exist among train movements. The improved CA model is proposed with respect to the moving-block railway system which operates under the condition that the states (position and speed) of particles (trains) are known.

The paper is organized as follows. Section 2 summarizes the principle of moving-block system and other tempo-spatial constraints influencing the dynamics of train movement. Section 3 develops the improved model under some fundamental tempo-spatial constraints. The simulation results are demonstrated and elucidated in section 4. Finally, the conclusions are drawn in section 5.

## 2 Train movement dynamics

### 2.1 Moving-block system

The recent tremendous advancement of information and communication technology has pushed forward the implementation of moving-block system through providing the accurate positioning information for high-speed locomotives. It has been implemented in urban rail transit and some contemporary communication-based railway lines. Compared with fixed-block system, the moving-block one can achieve high density and capacity of transportation.

Fig. 1 sketches the mechanism of moving-block system. Several types of moving-block systems were discussed by Pearson (1973) such as moving space block (MSB), moving time block (MTB) and pure moving block (PMB). MSB simply adopts the minimum instantaneous distance  $d_n$  of train  $n$  with sufficient margin between successive trains as:

$$d_n = v_{\max}^2 / (2b) + SM \quad (1)$$

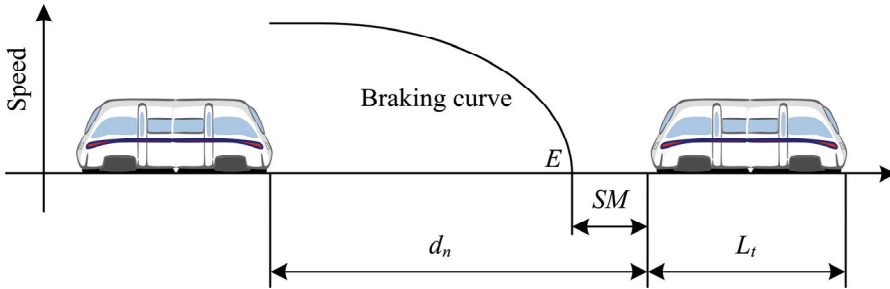


Figure 1: The mechanism of moving-block system.

where  $v_{max}$  is the maximum velocity of train,  $b$  is the deceleration and  $SM$  is the safety margin distance.

PMB allows adjusting the minimum instantaneous distance according to the current speed  $v_f$  of following train, i.e.

$$d_n = v_f^2 / (2b) + SM. \quad (2)$$

However, MTB adopts the minimum instantaneous distance intervenient to those of MSB and PMB, i.e.

$$\begin{aligned} d_n &= v_{max} v_f / (2b) + SM \\ &= v_f / v_{max} \cdot (v_{max}^2 / (2b)) + SM \\ &= v_f \cdot d_{max} / v_{max} + SM \end{aligned} \quad (3)$$

where  $d_{max}$  is the braking distance when train decelerates from  $v_{max}$  to 0 at the rate of  $b$ . From Eq. 3, we can learn that MTB purposes to realize the interval (headway) between two trains passing any point along the line is always constant and independent of running speed.

The performance of MSB, MTB and PMB has been extensively studied, which shows that PMB gives the best performance and is the basis of all currently implemented systems [Takeuchi, Goodman, and Sone (2003)]. The discussion of this paper is with regard to PMB, but the concept is extensible for MSB and MTB.

## 2.2 Other tempo-spatial constraints

### 2.2.1 Scheduled movement authority

Movement authority (MA) is the distance that a train is allowed to travel before it is required to stop or reduce its speed to a certain value. This information can be

calculated based on the interlocking and track status and positioning information. In addition, scheduling commands also specify MA, called scheduled MA (SMA), in exceptional circumstances. Fig. 2 demonstrates two kinds of typical SMAs. Fig. 2(a) shows the case that train  $j$  runs according to SMA, which happens at section in railway network. Train  $j$  and  $k$  belongs to the same line, while train  $i$  the other line. Two lines have the common part. When train  $i$  enters into the common part, train  $j$  will immediately regard train  $i$  as its front adjacent one and run according to the new minimum instantaneous distance  $d_j$ . In this case,  $d_j$  might be subject to abrupt change, and thus train  $j$  would suffer from abrupt braking and even collision if there is no SMA. Fig. 2(b) displays the circumstance that train  $i$  should wait at station although its departure time is due for train  $j$ 's first departure or stop at station to wait for train  $j$ 's preferential passing through, which often happens in order to improve the operation performance of total railway network. Here, we regard the scheduled waiting at station as a special case of scheduled MA, while the scheduled stop at station is similar to the case described in Fig. 2(a).

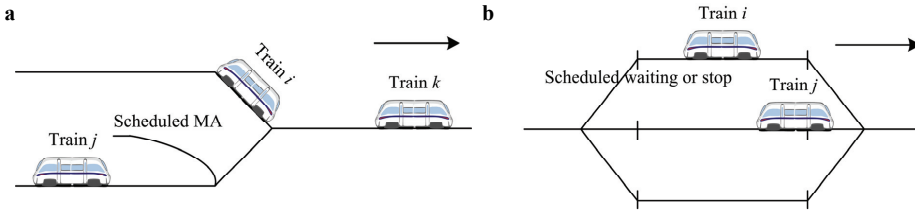


Figure 2: Scheduled movement authority. (a) at section, and (b) at station.

### 2.2.2 Speed constraints

Train dynamics is restrained by various factors such as maximum speed restriction profile, static speed profile (SSP), mode-related speed restriction and temporary speed restriction (TSR) which engender most restrictive speed profile (MRSP) as shown in Fig. 3. SSP is the specification of fixed speed restriction for a segment of track line, related to the line condition such as gradient, curvature and adhesion coefficient of track. Train operation mode is the way with corresponding level to control train. There exist different speed ranges for different operation modes. TSR is issued under exceptional case such as bad weather and certain equipment failure. MRSP adopts the minimum value among all kinds of speed restrictions. When train runs from low- to high-level speed restriction, it should not be executed until the total body of train has passed through the restricted segment with low-level speed limit.

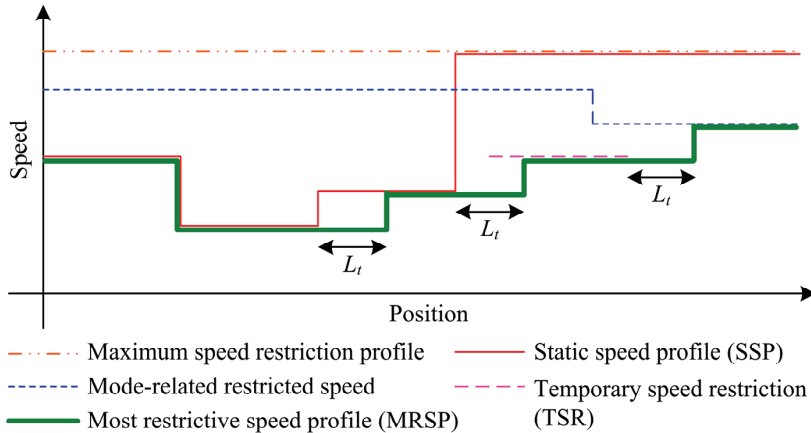


Figure 3: The formation of most restrictive speed profile.

### 3 Proposed model

#### 3.1 Basic CA model for railway traffic

The basic CA model has been proposed for moving-block railway traffic [Li, Gao, and Ning (2005a, 2005b)] in two cases that train runs after another one and towards station. Here, we unify them into the following form for simplicity:

Step 1 acceleration:

```

if  $\Delta x > d$ ,  $v_n = \min(v_n + a, v_{max})$ 
elseif  $\Delta x < d$ ,  $v_n = \min(v_n - b, 0)$ 
else  $v_n = v_n$ 
end
  
```

Step 2 slowing down:

$$v_n = \min(v_n, gap)$$

Step 3 movement:

$$x_n = x_n + v_n$$

where  $\Delta x$  denotes the distance headway from train  $n$  to its front adjacent one or that from train  $n$  to its front adjacent station, and  $d$  represents the minimum instantaneous distance  $d_n$  or the distance that train  $n$  can enter station through deceleration. The corresponding value is assigned according to whether train's running after another one or towards station.  $v_n, v_{max}$ ,  $a$ ,  $b$ , and  $x_n$  are the speed, the maximum speed, the acceleration, the deceleration, and the position of train  $n$ , respectively.

### 3.2 Proposed model

In order to establish the generalized model of train movement with various tempo-spatial constraints for the moving-block system, we define three kinds of target points:

- (1)  $p_a$ : the desired stop point of a train if its preceding train comes to a sudden halt (see point  $E$  in Fig. 1). Especially, if the front is station, the desired stop point is the station. The speed limit  $v_a$  at that point is generally set to be 0.
- (2)  $p_b$ : the end point of a speed-restriction segment of MRSP where the speed limit  $v_b$  is the minimum value among all kinds of speed restrictions at that point (see Fig. 3).
- (3)  $p_c$ : the end point specified by the SMA where the speed limit  $v_c$  can be specified as 0 or a certain value (see Fig. 2). If  $v_c \neq 0$ , we especially call SMA the scheduled limit of MA (SLMA).

Suppose that the distances from a train to the above three kinds of target points are  $d_a$ ,  $d_b$ , and  $d_c$ , respectively. We suppose that  $p_b$  always exists, and moreover dynamically updates. If there exists  $p_c$ , MA can be determined by:

$$d_m = \min(d_a, d_c). \quad (4)$$

However, SMA has its life cycle. Let  $LC(sc)=1$  denote the SMA is still active and  $LC(sc)=0$  inactive. In order to avert any value of  $d_c$  when SMA is inactive, Eq. 4 should be revised as:

$$d_m = \min(d_a, d_c) \cdot LC(sc) + d_a \cdot (1 - LC(sc)). \quad (5)$$

In view of current instant, if there exists  $p_c$ , the distance from train's current position to the nearest target point  $p_t$  is defined as:

$$d_t = \min(d_a, d_b, d_c). \quad (6)$$

where this  $p_t$  is also called the instantaneous target point, and correspondingly  $d_t$  is called the instantaneous MA. Considering the life cycle of SMA, Eq. 6 should be revised as:

$$d_t = \min(d_a, d_b, d_c) \cdot LC(sc) + \min(d_a, d_b) \cdot (1 - LC(sc)). \quad (7)$$

Given the speed  $v_t$  at the target point  $p_t$ , the distance  $d_t$  from train's current position to  $p_t$ , and the allowable deceleration rate  $b$ , in order to abstain from exceeding the speed limit at  $p_t$ , the current speed  $v_c$  of train should be controlled below:

$$v_r = \sqrt{2bd_t + v_t^2}. \quad (8)$$

We call the curve engendered by Eq. 8 the basic speed limit one. From Eq. 8, we can directly obtain the following proposition.

**Proposition 1:** If at certain instant, train's current speed  $v_c$  and its distance  $d_t$  to the target point  $p_t$  satisfy Eq. 8, the train can arrive at  $p_t$  with the target speed  $v_t$  at the deceleration of  $b$  if there is no other speed restriction.

From proposition 1, we can derive that when  $v_c$  is located below the basic speed limit curve, train can accelerate, keep current speed and decelerate. What state the train will on earth locate at is determined by  $d_t$ . The NaSch CA model denotes the velocity as the displacement of a particle at next simulation step. Taking this into account, proposition 2 follows.

**Proposition 2:** Suppose that the deceleration rate is  $b$ , the position to the nearest target point is  $d_t$ , the corresponding target speed is  $v_t$ , and the current speed is  $v_c$ .

- (a) If  $d_t > (v_c^2 - v_t^2)/(2b) + v_c$ , train can accelerate,
- (b) if  $d_t = (v_c^2 - v_t^2)/(2b) + v_c$ , train can keep the current speed  $v_c$ , and
- (c) if  $d_t < (v_c^2 - v_t^2)/(2b) + v_c$ , train will decelerate to  $v_t$ .

Recall that there exists MRSP. We denote it as  $v_{\lim}(x)$  where  $x$  is the position at which train locates on the track line. In practice, if train's velocity is over the speed limit, the train will be ready to decelerate, which is called a process of automatic train protection (ATP). If train's velocity does not exceed the speed limit, the train might accelerate, hold the current speed or decelerate as proposition 2 describes. Considering the various factors of speed restriction and the position relationship among  $d_a$ ,  $d_b$  and  $d_c$ , the target speed  $v_t$  is determined by:

$$v_t = \min(v_{\lim}(x_t), \sqrt{2b(d_a - d_t)}, \sqrt{2b(d_c - d_t) + v_c^2}, \sqrt{2b(d_b - d_t) + v_b^2}, v_{\max}) \cdot LC(sc) + \min(v_{\lim}(x_t), \sqrt{2b(d_a - d_t)}, \sqrt{2b(d_b - d_t) + v_b^2}, v_{\max}) \cdot (1 - LC(sc)) \quad (9)$$

where  $x_t$  is the position of  $p_t$ , and  $v_{\max}$  is the maximum speed of train. Define that  $x_c$  and  $x_{c+1}$  are the positions at current and next instant, respectively.  $v_{c+1}$  is the velocity at next instant, and  $a$  is the acceleration rate. The CA model of train movement incorporating tempo-spatial constraints is described as follows:

#### (1) Speed update

$$\begin{aligned} &\text{if } v_c > v_{\lim}(x_c), v_{c+1} = \max(v_c - b, 0) \\ &\text{elseif } v_c = v_{\lim}(x_c) \text{ AND } d_t \geq (v_c^2 - v_t^2)/(2b) + v_c, \end{aligned}$$

$$v_{c+1} = v_c$$

```

else
  if  $d_t > (v_c^2 - v_t^2)/(2b) + v_c$ ,  $v_{c+1} = \min(v_c + a, v_{\max})$ 
  elseif  $d_t = (v_c^2 - v_t^2)/(2b) + v_c$ ,  $v_{c+1} = v_c$ 
  else
    if  $v_c = v_t \neq 0$ ,  $v_{c+1} = v_c$ 
    else  $v_{c+1} = \min(\max(v_c - b, v_t), d_m)$ 
  end
end
end
end
    
```

(2) Position update

$$x_{c+1} = x_c + v_{c+1}$$

In the above model, the detectable current speed  $v_c$  is explicitly incorporated into the estimation of the instantaneous braking reference distance, denoted as  $d_r$ . Besides, the acceleration, hold and deceleration involve the manipulation of MRSP and SMA. The driver or the driving equipment of train is always judging if  $v_c$  exceeds the speed limit  $v_{\text{lim}}(x_c)$  and enquiring if  $v_c$  can be decelerated to the target speed  $v_t$  with the distance  $d_t$  to the current (instantaneous) target point  $p_t$ . The basic idea of the model is firstly to judge the tendency of speed update, secondly to update the speed. This procedure is repeated according to the feedback of  $v_c$  and  $d_t$ . The model is of feedback adjustment of speed, which can be observed in practice. It should be noted that the acceleration  $a$ , related to  $d_t$ ,  $d_r$ ,  $v_c$  and so on, is determined by control strategies.

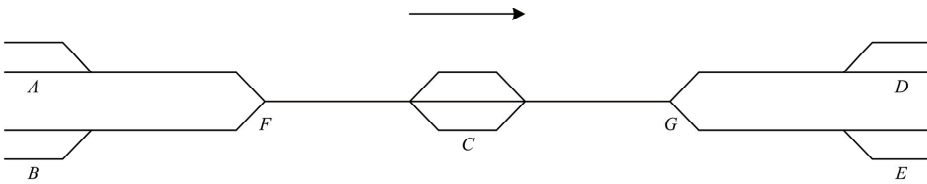


Figure 4: Railway network.

#### 4 Simulation results

The simulated railway network is shown in Fig. 4. The network has five stations, i.e.  $A$ ,  $B$ ,  $C$ ,  $D$  and  $E$ . Two transport lines, line 1 and 2, are designed in this simulation. Line 1 and 2 are from station  $A$  to  $E$  and  $B$  to  $D$ , respectively, passing through junction  $F$  and  $G$  and with a stop at station  $C$ . Only one platform is employed at

the first and last stations for line 1 and 2, and two platforms are provided at station *C* for the common use of two lines. The length of track segment *AF*, *BF*, *FC*, *CG*, *GD* and *GE* is 2500m, 1500m, 3000m, 3000m, 1500m, and 2500m, respectively. The length of each cell is 1m. The maximal speeds of trains along line 1 and 2 are  $v_1^{\max}=30\text{cells/s}$  and  $v_2^{\max}=20\text{cells/s}$ , i.e. 108km/h and 72km/h, respectively. The acceleration and deceleration rates are  $a=1\text{cell/s}^2$  and  $b=1\text{cell/s}^2$  (in absolute value), respectively. The dwell time at each station for line 1 and 2 is  $T_d=60\text{s}$ . There are speed-restricting segments with a length of 600m and centering on junction *F* and *G* for line 1 and line 2, respectively, whose speed limits are both set to be 11cells/s, i.e. 40km/h. The simulation step is set as 1s, and the maximal simulation time is 7200s. The train length  $L_t=90\text{m}$  and the safety margin distance  $SM=10\text{m}$ . The simulation records the position of train head as that of the whole train. The railway network operates in the moving-block way.

#### 4.1 $d_a$ and $d_b$ control

Both line 1 and 2 begin to dispatch train at instant 0, and the interval of departure time  $T_i$  is 300s. 24 trains are dispatched for line 1 and 2, respectively. SMA is not applied to this simulation test, and only  $d_a$  and  $d_b$  manipulate the train movement. Fig. 5 demonstrates the tempo-spatial dynamics. Fig. 5(a) and (b) show that slow trains on line 2 lead fast trains on line 1 to run on the common sections. The trajectories starting from junction *F* and ending at junction *G* are those of trains belonging to line 2 and ones line 1 in Fig. 5(a) and (b), respectively. Fig. 5(c) and (d) display that the train movement is composed of several main components, i.e. accelerating when train departs from station, holding when its speed reaches the maximum one, decelerating when it prepares to enter into the speed-limit segment or station, and re-holding when its speed reaches the designated one. Because the fast train will catch up with and track the slow one, the tracking procedures and the steady states can be observed from the movements before station *C* and junction *G*, respectively, in Fig. 5(c) and (d). Fig. 5(e) and (f) are the decomposition of Fig. 5(c), as an example. The similar decomposition can be attained for the remained plots of the relationship among speed, position and time in this paper.

Fig. 6 expounds how  $d_a$  and  $d_b$  maneuver the train movement, setting the first trains of line 1 and 2, No. 1001 and 2001 as an example. Fig. 6(a) shows the plots of position versus time for train 1001 and 2001 as well as the projection of trajectory of train 2001 on line 2 onto line 1. Train 2001 enters into the common segment at instant 160s, arrives at station *C* at instant 335s (point *J* in Fig. 6(a)), and leaves the common segment at instant 570s. If there is no other train in front of the current train, the train will set the front adjacent station as  $p_a$ , as shown in Fig. 6(b) at the intervals of [0, 159s], [335s, 395s] and [570s, 711s].  $d_f$  in Fig. 6(b) represents the

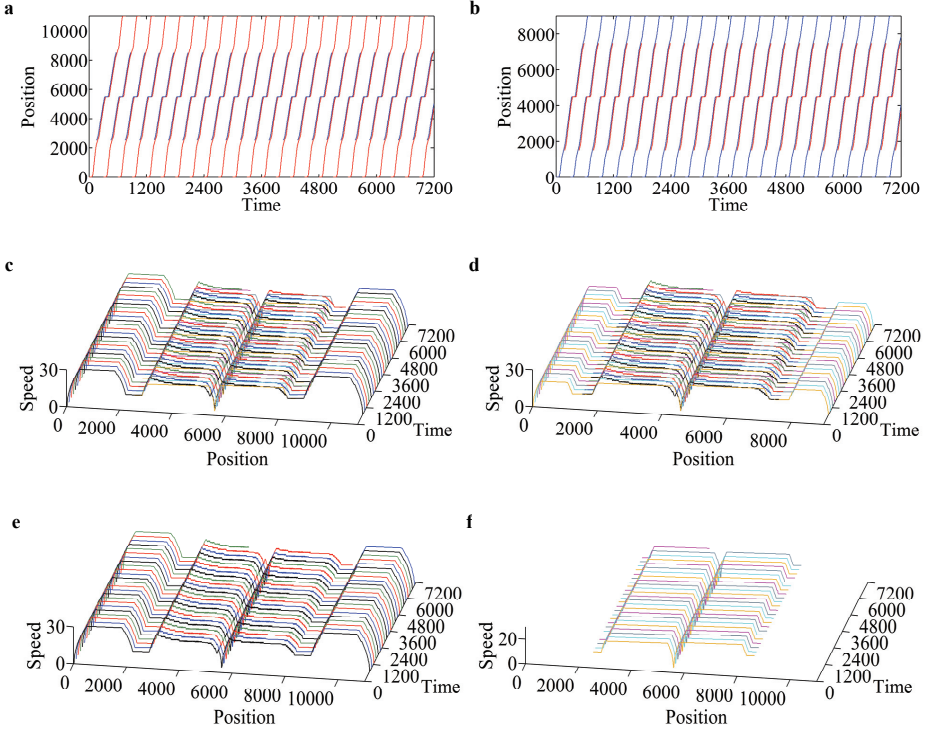


Figure 5: Tempo-spatial dynamics. (a) and (b) are plots of position and time for line 1 and 2, respectively. (c) and (d) are spots of speed, position and time for line 1 and 2, respectively. (e) and (f) are plots of speed, position and time for trains running on line 1 but belonging to line1 and 2, respectively.

difference between positions of train 2001 and 1001.  $d_a$  in Fig. 6(b) is basically consistent with  $d_f$  subtracting  $L_t$  and  $SM$ . However, there is a leap at point  $M$  in Fig. 6(b), and thus point  $N$  in Fig. 6(d), which is because Train 2001 has entered into station  $C$  at that time. In addition, if  $d_f \leq L_t + SM$ ,  $d_a=0$ , which is required by PMB. Train 1001 enters into the speed-restricting segments at instant 155s and 561s (point  $H$  and  $K$  in Fig. 6(a), respectively), and leaves them at instant 210s and 616s (point  $I$  and  $L$  in Fig. 6(a), respectively). Train 1001 arrives at station at instant 354s. Thus, the leaps can be observed in Fig. 6(c) at instant 155s, 210s, 354s, 561s and 616s, which implies new  $p_b$ s appear. Fig. 6(d) shows the plot of  $d_t$  versus time, which eventually controls the train movement according to the proposed rule of speed update. Fig. 6(e) depicts the variation process of speed with time. There is

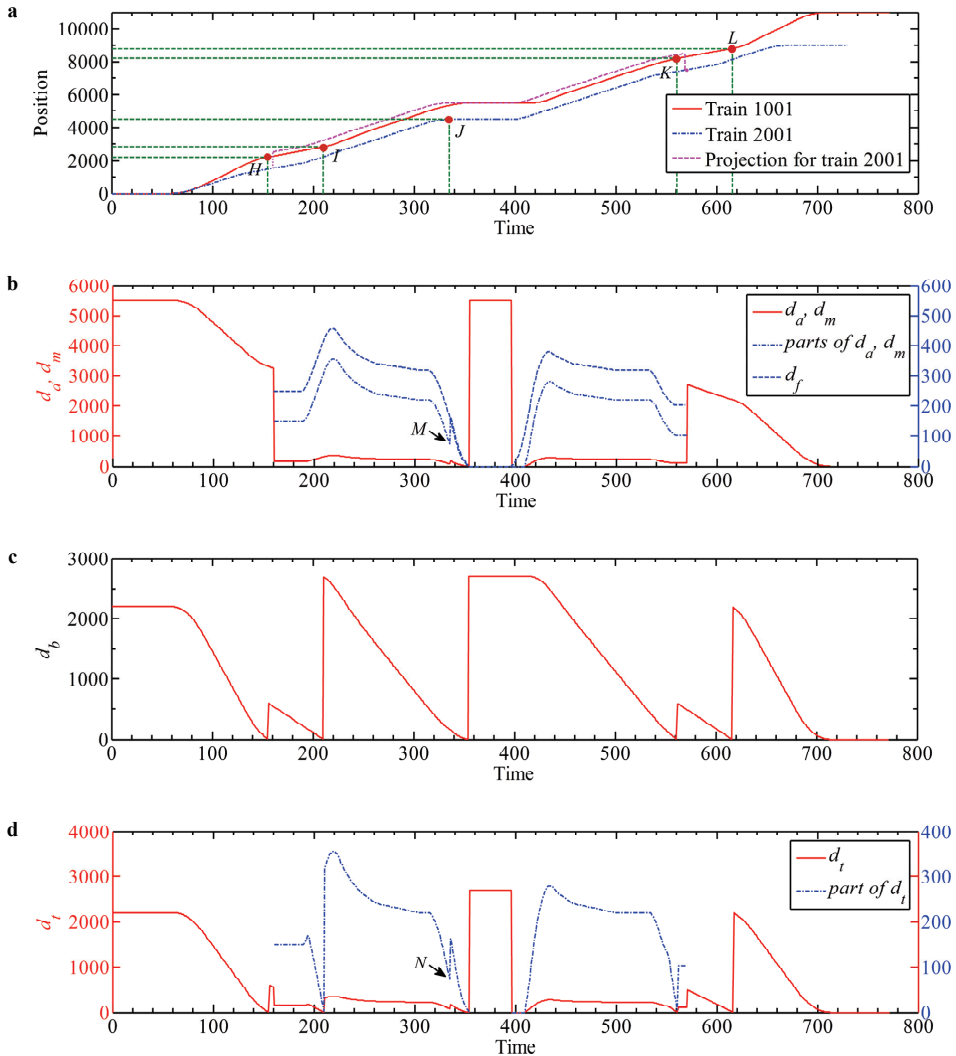


Figure 6: Tempo-spatial dynamics for train 1001. (a) plot of position and time for train 1001 and 2001. (b), (c), and (d) are plots of  $d_a$  and  $d_m$ ,  $d_b$ , and  $d_t$  versus time for train 1001, respectively. (e) plot of speed and time for train 1001.

speed fluctuation when train 1001 follows train 2001, which simulates the feedback adjustment process. When the speed of train 1001 decreases to the same as that of train 2001, and moreover the distance between trains' heads equals to  $L_t + SM + d_r$ , the tracking process will approach to the steady state. When train 2001 begins

to decelerate, the speed of train 1001 will descend in an undulated way. There is chance of speed ascendance at point  $O$  in Fig. 6(e), which is because  $d_t$  abruptly increases by  $L_t+SM$ .

Here, the mechanism of speed fluctuation is elucidated. Tab. 1 lists the partial parameters concerning the calculation of train speed from instant 225s to 305s in Fig. 6. POT2 represents the position of train 2001 on line 2, and POT1 denotes the position of train 1001 on line 1. At the instant of 225s, because  $d_t < d_r$ , the speed will decrease by 1 at next instant. However, at instant 228s, the speed will be increased by 1 because  $d_t > d_r$  at the previous instant. The similar analysis can be undertaken to justify the speed variation.

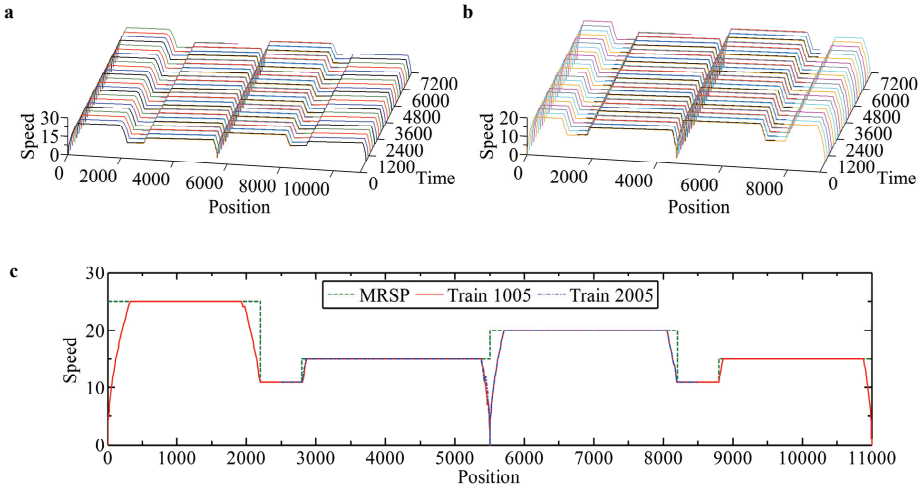


Figure 7: Multi-segment speed restriction. (a) plot of speed, position and time for line 1, (b) plot of speed, position and time for line 2, and (c) a sampling plot of speed and position.

Fig. 7 displays the simulation results of multi-segment speed restriction on line 1. The MRSP is plotted in Fig. 7(c). Because the speeds of trains are confined to a certain scale so that the maximum allowable speeds are the same for both lines, little speed fluctuation can be observed for the trains on the common segments, similar to the speed dynamics on the non-common segments.

Table 1: The parameters related to train movement.

Time	225	226	227	228	229	...	299	300	301	302	303	304	305
POT 2	2528	2548	2568	2588	2608	...	4008	4028	4048	4068	4088	4108	4128
POT 1	3093	3118	3142	3167	3191	...	4686	4707	4727	4748	4768	4788	4808
$d_u, d_m$	335	330	326	321	317	...	222	221	221	220	220	220	220
$d_b$	2407	2382	2358	2333	2309	...	814	793	773	752	732	712	692
$d_t$	335	330	326	321	317	...	222	221	221	220	220	220	220
$d_r$	364	337	312	337	312		220	241	220	241	220	220	220
Speed	26	25	24	25	24	...	20	21	20	21	20	20	20

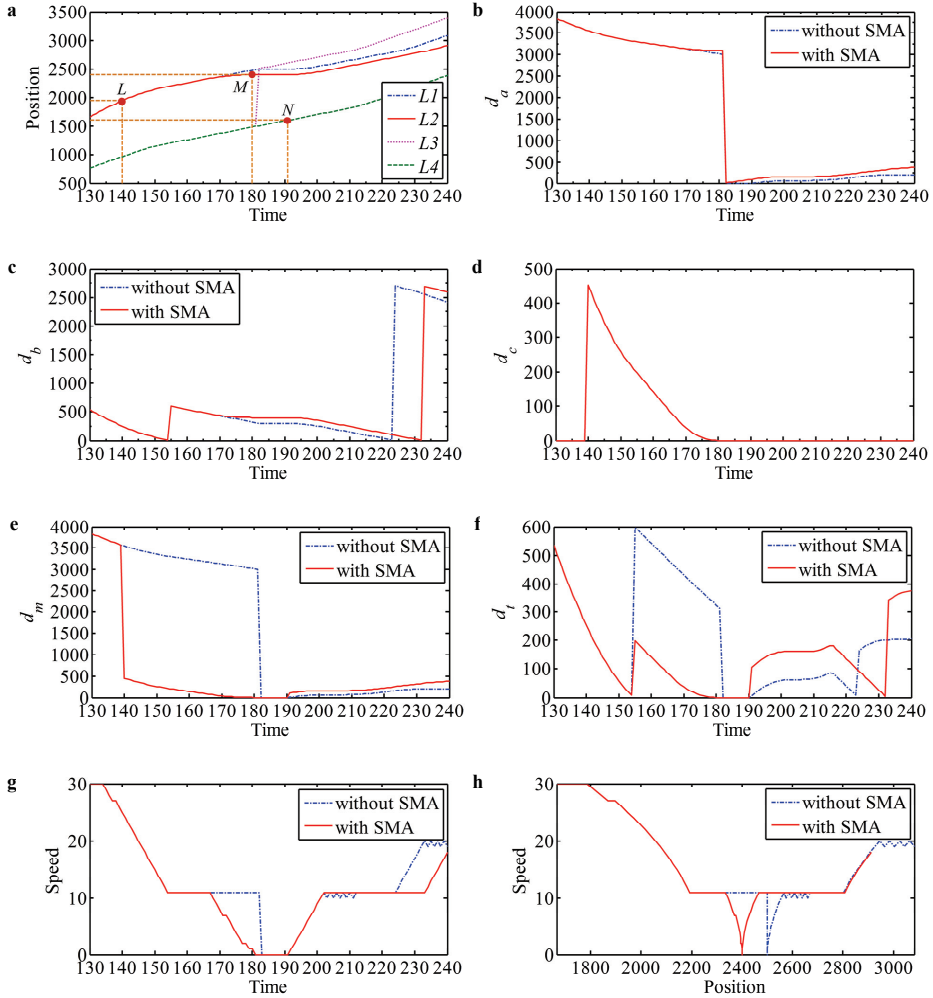


Figure 8: Tempo-spatial dynamics without and with SMA. (a) plot of position versus time for train 1001 and 2001 (L1: train 1001 without SMA, L2: train 1001 with SMA, L3: projection of trajectory of train 2001 onto line 1, L4: train 2001). (b), (c), (e) and (f) are plots of  $d_a$ ,  $d_b$ ,  $d_m$  and  $d_t$  versus time without and with SMA. (d) is plot of  $d_c$  versus time. (g) and (h) are plots of speed versus time or position without and with SMA.

#### 4.2 $d_a$ , $d_b$ and $d_c$ control

In order to observe the abrupt speed declination at junction  $F$  affected by the trains on the other line, we make the first train of line 2 depart at instant 22s. Fig. 8

demonstrates the tempo-spatial dynamics of train 1001 without and with SMA. From Fig. 8 (a), we can notice that train 2001 will pass junction  $F$  at instant 182s, which will cause the abrupt changes of  $d_a$  and thus  $d_m$  and  $d_t$  as shown in Fig. 8(b), (e) and (f), respectively. At this case,  $d_a$  can not make train 1001 move anymore, and steep speed descent can be observed in Fig. 8(g) and (h) without SMA. The deceleration rate of  $11\text{cells/s}^2$  in Fig. 8(g) and (h) is on one hand an unrealistic deceleration (generally less than the gravitational acceleration), and on the other hand far beyond the one at which passengers feel comfortable (less than  $3\text{-}4\text{m/s}^2$  [Moon, Moon, and Yi (2009)]), not to mention this case without SMA is very dangerous. If we set  $p_c$  at the position of  $2400\text{cells}$  ( $=AF-L_t-SM$ ) for SMA, thus the position from which place train can just decelerate at the rate of  $b$  from  $v_1^{\max}$  to 0 is  $1950\text{cells}$  ( $=AF-L_t-SM-v_1^{\max} \times v_1^{\max}/2$ ). At instant 140s, train 1001 arrives at the position of  $1947\text{cells}$ , just less than  $1950\text{cells}$  (point  $L$  in Fig. 8(a)). At this instant, the SMA is set to be active as shown in Fig. 8(d). When train 1001 runs according to the SMA, it will arrive at  $p_c$  at instant 180s (point  $M$  in Fig. 8(a)), and at this time  $d_c$  will approach 0 again. Train 2001 leaves the position with a distance to junction  $F$  just greater than  $L_t+SM$  at instant 191s, it is the time that the SMA is set inactive in order not to influence the transport efficiency. Fig. 8(c) displays the phenomena that when train 1001 enters into a new speed-restricting segment, there will be precipitous change for  $d_b$ . Once the SMA is set at instant 140s, there will be new target point  $p_c$  for  $d_m$  as shown in Fig. 8(e). The synthetic  $d_t$  as shown in Fig. 8(f) from  $d_a$ ,  $d_b$  and  $d_c$  controls the train movement and makes train steadily run towards and finally stop at  $p_c$  as shown in Fig. 8(g) and (h).

We design the comprehensive simulation to test the proposed model applicable for the SMA at section and station as shown in Fig. 2. We first detect the potential conflict [Mazzarello and Ottaviani (2007); D'Ariano, Pacciarelli, and Pranzo (2007)] at junction  $F$  when one train just passes the junction, which will cause the train and its front adjacent one to locate within  $L_t+SM$ . If conflict happens, two scheduling strategies are adopted. One is to give priority to the train which arrives at junction  $F$  first, and the other is to give priority to the train which is faster. These two strategies are corresponding to case I and II, respectively. We design case III based on case I, i.e. arranging the scheduled MA at station for slow train to give priority to the successive fast train.

Fig. 9 and Fig. 10 reveal the tempo-spatial dynamics under the above three cases with  $T_i=300\text{s}$  and  $90\text{s}$ , respectively. Under case I, slow trains belonging to line 2 lead fast ones belonging to line 1 to advance on the common segments as shown in Fig. 9(a) and Fig. 10(a). From Fig. 9(c) and Fig. 10(c), we can learn that, under case II, fast trains belonging to line 1 lead slow ones belonging to line 2 to run on those common segments. Under case III, the compromise appears as shown

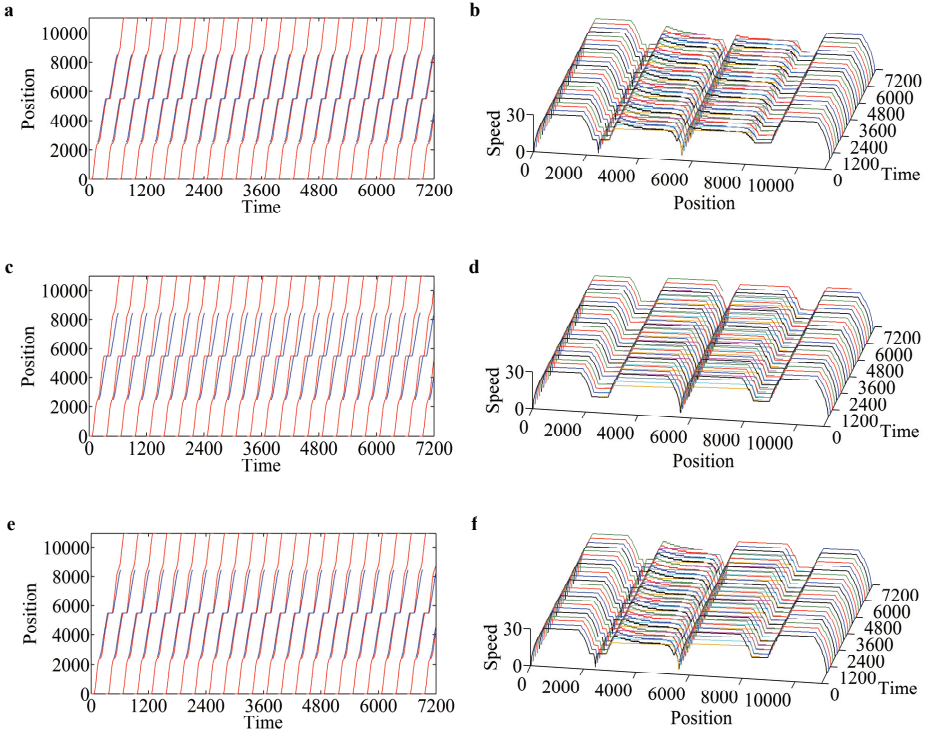


Figure 9: Tempo-spatial dynamics with SMA at section and station ( $T_i = 300s$ ). (a) and (b) are for case I. (c) and (d) are for case II. (e) and (f) are for case III.

in Fig. 9(e) and Fig. 10(e). Before station  $C$ , slow trains lead fast ones, however after station  $C$ , and it is just the reverse.

Comparing Fig. 9(b) with Fig. 10(b), we can observe the phenomenon that the fast trains chase after and follow the slow ones until the steady state is approached. Although the speed variation is flattened before station  $C$  in Fig. 9(d) and Fig. 10(d), however, after station  $C$ , there exists the tracking phenomenon in Fig. 10(d), which is because the density is so high when  $T_i=90s$  compared with that when  $T_i=300s$ , the speeds of fast trains have to decrease to follow the front adjacent slow ones. There exists no stop at  $p_c$  before junction  $F$  in Fig. 9(d) and Fig. 10(d). The reason accounting for this phenomenon is that before slow trains arrive at  $p_c$ , fast trains have left the place with a distance of  $L_t+SM$  to junction  $F$  at the moment the SMA should be cancelled. There exists speed descent for fast trains to track the leading slow ones before station  $C$ , but after station  $C$ , the leading fast train can run

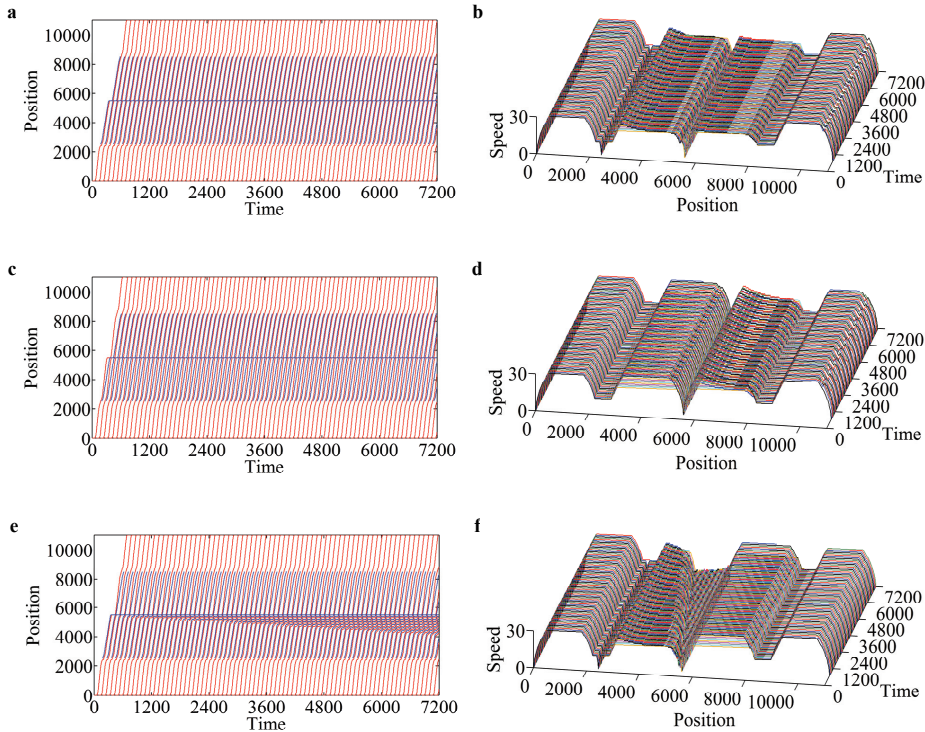


Figure 10: Tempo-spatial dynamics with SMA at section and station ( $T_i = 90s$ ). (a) and (b) are for case I. (c) and (d) are for case II. (e) and (f) are for case III.

towards and at the maximum speed, as shown in Fig. 9(f). Because of high density and great delay caused by scheduled waiting in Fig. 10(f), before station C, the go-and-stop wave and its back propagation to the upstream can be observed. Fast trains can run towards and at the maximum speed after station C because they lead the slow trains to run and however, their distances to the front adjacent slow trains do not impede them to accelerate to the maximum value.

## 5 Conclusions

The CA model is composed of four basic components, i.e. physical environment, cell's states, cell's neighborhoods and update rules. It integrates the description of dynamics of cells themselves with those of interactions among cells, which are reflected in the update rules. Under this basic framework, this paper has proposed an improved CA model for moving-block railway network considering the tempo-

spatial constraints to describe the constrictive and cooperative movements among cells. The tempo-spatial constraints constitute the real ( $p_a$ ) and dummy neighborhoods ( $p_b$  and  $p_c$ ) of cells, and control the dynamics of state transition (limit at each step). Through the proposed model, we can observe the phenomenon of stop-and-go wave, its back propagation to the upstream and speed tracking adjustment based on the feedback of distances to the real and dummy neighborhoods. The movement mechanism and the rationality of simulated results are explicated under the control of real and dummy neighborhoods.

Computer simulation of train movement about the relationship among trains' position, speed and time, i.e. tempo-spatial dynamics, in railway network plays very important role in planning, real-time decision and plan adjustment for train operation in contemporary computer-assisted decision system. The proposed CA model in this paper has incorporated the physical law of individual train movement into the local interactions among cells. This paper aims to propose the generalized description of train movement without setting adjustable parameters such as acceleration  $a$  and deceleration  $b$  related to the concrete control strategies. With regard to certain control strategy such as energy-efficient control [Liu, Golovitcher (2003)], our model still requires further perfecting, which will be left for future research.

**Acknowledgement:** This work is supported by the Fundamental Research Funds for the Central Universities of China (Grant No. 2009JBM006) and the National Natural Science Foundation of China (Grant No. 61074138).

## References

- Alizadeh, R.** (2011): A dynamic cellular automaton model for evacuation process with obstacles. *Saf. Sci.*, vol. 49, pp. 315-323.
- Blue, V. J.; Adler, J. L.** (2001): Cellular automata microsimulation for modeling bi-directional pedestrian walkways. *Transp. Res. B*, vol. 35, pp. 293-312.
- Cheng, Y.** (1998): Hybrid simulation for resolving resource conflicts in train traffic rescheduling. *Comput. Ind.*, vol. 35, pp. 233-246.
- Chou, M.; Xia, X.; Kayserb, C.** (2007): Modelling and model validation of heavy-haul trains equipped with electronically controlled pneumatic brake systems. *Control Eng. Pract.*, vol. 15, pp. 501-509.
- Chowdhury, D.; Santen, L.; Schadschneider, A.** (2000): Statistical physics of vehicular traffic and some related systems. *Phys. Rep.*, vol. 329, pp. 199-329.
- Chowdhury, D.; Wolf, D. E.; Schreckenberg, M.** (1997): Particle hopping models for two-lane traffic with two kinds of vehicles: effects of lane changing rules. *Physica A*, vol. 235, pp. 417-439.

**D'Ariano, A.; Pacciarelli, D.; Pranzo, M.** (2007): A branch and bound algorithm for scheduling trains in a railway network. *Eur. J. Oper. Res.*, vol. 183, pp. 643-657.

**Fu, Y.-P.; Gao, Z.-Y.; Li, K.-P.** (2007): The characteristic analysis of the traffic flow of trains in speed-limited section for fixed-block system. *Acta Phys. Sin.*, vol. 56, pp. 5165-5171.

**Grube, P.; Núñez, F.; Cipriano, A.** (2011): An event-driven simulator for multi-line metro systems and its application to Santiago de Chile metropolitan rail network. *Simul. Model. Pract. Th.*, vol. 19, pp. 393-405.

**Higgins, A.; Kozan, E.** (1998): Modeling train delays in urban networks. *Transport. Sci.*, vol. 32, pp. 346-357.

**Ho, T. K.; Mao, B. H.; Yang, Z. X.** (1998): A multi-train movement simulator with moving block signalling. *WIT Trans. on the Built Environ.: Comput. in Railways VI*, WIT Press, pp. 782-791.

**Li, F.; Gao, Z.-Y.; Li, K.-P.** (2007): Analysis of the property of train flow in the fixed autoblock systems. *Acta Phys. Sin.*, vol. 56, pp. 3158-3165.

**Li, K. P.; Gao, Z. Y.; Ning, B.** (2005a): Cellular automaton model for railway traffic. *J. Comp. Phys.*, vol. 209, pp. 179-192.

**Li, K. P.; Gao, Z. Y.; Ning, B.** (2005b): Modeling the railway traffic using cellular automata model. *Int. J. Mod. Phys. C*, vol. 16, pp. 921-932.

**Li, K.; Gao, Z.** (2007): An improved equation model for the train movement. *Simul. Model. Pract. Th.*, vol. 15, pp. 1156-1162.

**Li, K.-P.; Gao, Z.-Y.; Mao, B.-H.** (2007): Energy-optimal control model for train movements. *Chinese Phys.*, vol. 16, pp. 359-364.

**Li, K. P.; Gao, Z. Y.; Yang, L. X.** (2007): Modeling and simulation for train control system using cellular automata. *Sci. China Ser. E- Tech. Sci.*, vol. 50, pp. 765-773.

**Liu, R.; Golovitcher, I.** (2003): Energy-efficient operation of rail vehicles. *Transp. Res. A*, vol. 37, pp. 917-932.

**Lu, Q.; Dessouky, M.; Leachman, R.C.** (2004): Modeling train movements through complex rail networks. *ACM. Trans. Mod. Comput. Sim.*, Vol. 14, pp. 48-75.

**Maerivoet, S.; Moor, B. D.** (2005): Cellular automata models of road traffic. *Phys. Rep.*, vol. 419, pp. 1-64.

**Mazzarello, M.; Ottaviani, E.** (2007): A traffic management system for real-time traffic optimisation in railways. *Transp. Res. B*, vol. 41, pp. 246-274.

- Meng, J.-P.; Dai, S.-Q.; Dong, L.-Y.; Zhang, J.-F.** (2007): Cellular automation model for mixed traffic flow with motorcycles. *Physica A*, vol. 380, pp. 470-480.
- Moon, S.; Moon, I.; Yi, K.** (2009): Design, tuning, and evaluation of a full-range adaptive cruise control system with collision avoidance. *Control Eng. Pract.*, vol. 17, pp. 442-455.
- Nagel, K.; Raschke, E.** (1992): Self-organizing criticality in cloud formation? *Physica A*, vol. 182, pp. 519-531.
- Nagel, K.; Schreckenberg, M.** (1992): Cellular automaton models for freeway traffic. *Phys. I*, vol. 2, pp. 2221-2229.
- Ning, B.; Li, K. P.; Gao, Z. Y.** (2005): Modeling fixed-block railway signaling system using cellular automata model. *Int. J. Mod. Phys. C*, vol. 16, pp. 1793-1801.
- Pearson, L. V.** (1973): *Moving-block Signalling*. Ph.D. Thesis, Loughborough University of Technology, UK.
- Takeuchi, H.; Goodman, C. J.; Sone, S.** (2003): Moving block signalling dynamics: performance measures and re-starting queued electric trains. *IEE Proc. - Electr. Power Appl.*, vol. 150, pp. 483-492.
- Tang, T.; Li, K.-P.** (2007): Traffic modeling for moving-block train control system. *Commun. Theor. Phys.*, vol. 47, pp. 601-606.
- von Neumann, J.** (1966): *Theory of Self-Reproducing Automata*. University of Illinois Press.
- Xun, J.; Ning, B.; Li, K.-P.** (2007): Network-based train-following model and study of train's delay propagation. *Acta Phys. Sin.*, vol. 56, pp. 5158-5164.
- Xun, J.; Ning, B.; Li, K.-P.** (2009): Station model for rail transit system using cellular automata. *Commun. Theor. Phys.*, vol. 51, pp. 595-599.
- Zhou, H.-L.; Gao, Z.-Y.; Li, K.-P.** (2006): Cellular automaton model for moving-like block system and study of train's delay propagation. *Acta Phys. Sin.*, vol. 55, pp. 1706-1710.

